

Chapter 3

Application of the Pair Weight Method to the Las Campanas Redshift Survey with no Redshift Distortions

The power spectrum of matter in the universe can be used to measure the relevant parameters of models of the universe (*e.g.*, Eisenstein et al., 1999). Because galaxies are easily visible, it is common to use galaxies as a tracer for the underlying density field. It has been shown (Scherrer and Weinberg, 1998; Cole et al., 1988) that if galaxy formation is a local phenomenon, then the galaxy power spectrum on large scales is different from the mass power spectrum by a multiplicative constant (at least in the linear regime; Mann et al., 1998). This constant is the bias factor. Because of the expected similarities between the galaxy power spectrum and the mass power spectrum, it is not surprising that power spectra have been taken for all of the larger galaxy surveys.

Despite the wealth of measurements, the power spectrum on large scales is not yet well determined. Part of the problem lies in the fact that the redshift surveys have different selection criteria. For example, it is commonly thought (Peacock, 1997) that galaxies selected in the infrared may have a bias factor that is lower than those selected in the optical. Another problem is that the amount of data in each catalog still produces large (tens of percent) errors in the measurement of the power spectrum at any given wavenumber.

The Las Campanas Redshift Survey is one of the larger publicly available redshift surveys. The observational procedure maximized the number of galaxy redshifts given the telescope time available to the team. Although this maximization of the telescope time means

that the analysis will yield the highest possible number of galaxy redshifts, optimizing for the number of galaxy redshifts makes the analysis of the survey more difficult. Each of the 327 observing fields has a different covering factor. That is, one field may have redshifts for 85 percent of the galaxies where the next field over has redshifts for 65 percent of the galaxies. In addition to this, the catalog is 6 slices each having a width of 1.5° . This means that it is similar to 6 two-dimensional slices. This is a problem for analyses that rely on the measured wavelength to fit comfortably within the catalog (in any direction). These characteristics make the Las Campanas Redshift Survey difficult for traditional methods, yet an ideal catalog with which to test the pair weight compression method.

In chapter 2, we described a method for extracting the power spectrum from a redshift galaxy catalog. The pair weight compression method assigns weights to each galaxy pair within the catalog based on the selection function (the number of galaxies within the catalog divided by the true number of galaxies) of the catalog and the parameters that one wishes to measure. The method requires that the selection function of galaxies to be known for each position in the catalog. It does not require that the selection function have any particular properties (like being an angular selection function times a radial selection function). This means that the pair weight compression method should assign weights to the individual galaxy pairs to maximize the information extracted from the galaxy survey (given the limitation of the number of window functions available in the calculation). The LCRS certainly meets all requirements for the pair weight compression method.

In section 3.1 we discuss the modifications to the catalog that were made to make the analysis as accurate as possible. Section 3.2 describes the mathematics necessary to extract the power spectrum from the catalog using the pair weight method. In section 3.3 we extract the power spectrum from the LCRS. We then compare the results to power spectra from other works. We conclude in section 3.4

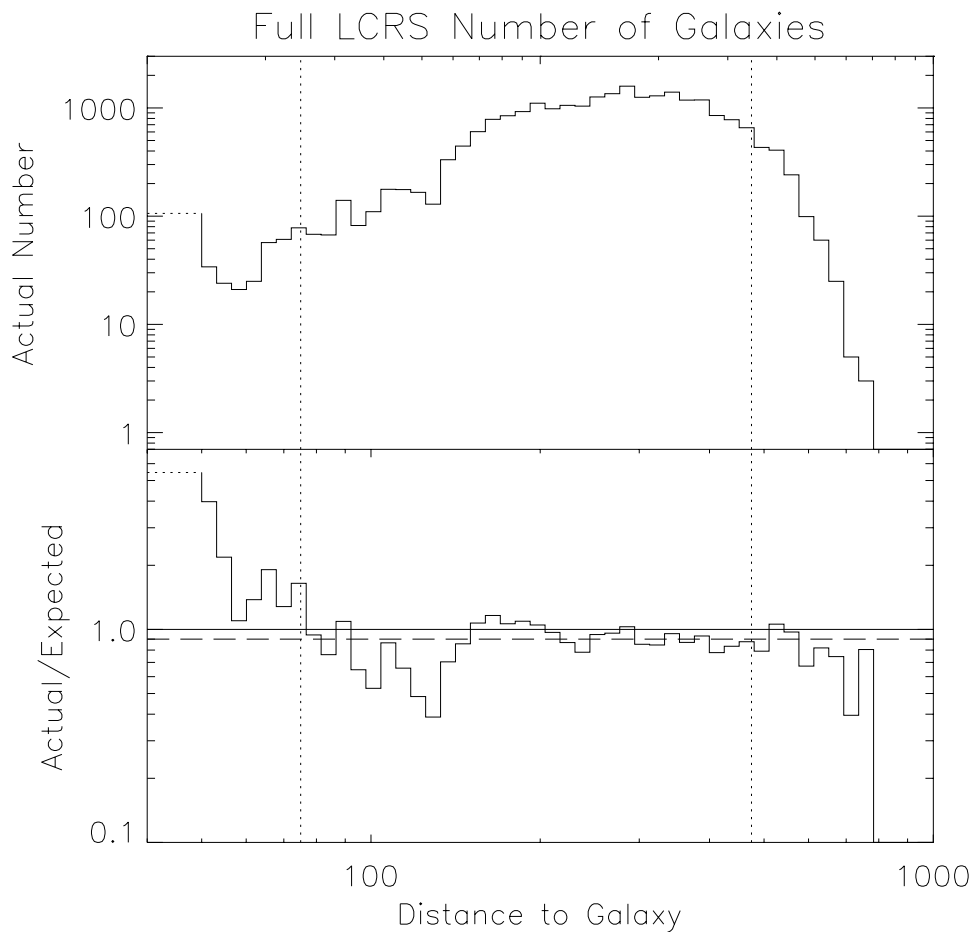


Figure 3.1: Top panel is the number of galaxies per logarithmic bin in the full Las Campanas Redshift Survey. The bottom panel shows the ratio of the number of galaxies in the full LCRS to the expected number based on the integrated selection function. The dashed line shows the ratio based on the total number of galaxies in the cut range divided by the number of galaxies found by integrating the selection function over the cut range.

3.1 Preparation of Catalog

The Las Campanas Redshift Survey (hereafter LCRS) of Shectman et al. (1996) contains 23720 galaxy redshifts stretching from $\sim 10h^{-1}$ Mpc to $\sim 800h^{-1}$ Mpc with the range of $75h^{-1}$ Mpc to $475h^{-1}$ Mpc being reasonably well sampled. Lin et al. (1996a) calculate the selection function of this well sampled region. The number of galaxies per logarithmic bin is shown in the top panel of Figure 3.1. In the lower panel is the ratio of the number of galaxies per

logarithmic bin to the expected number (using the selection function code generously provided by Huan Lin). This shows that the number of galaxies is well fit by the selection function in the region beyond $75h^{-1}$ Mpc.

In order to perform the calculations, we take two catalogs from the LCRS. The first is all 23720 galaxies, while the second is the 21996 galaxies between $75h^{-1}$ Mpc and $475h^{-1}$ Mpc. The lower cutoff is due to the fact that the selection function does not adequately describe the catalog below $75h^{-1}$ Mpc. The upper cut is because the catalog is rather sparse beyond this cut. This means that the statistics are not all that good. This means that the region beyond $475h^{-1}$ Mpc should not provide too much additional information.

3.2 Calculation of Power Spectrum

In chapter 2, we described how to extract the power spectrum from a galaxy survey using the pair weight compression method. The final result was that the estimate of ξ_β where β is the index of the separation is given by:

$$\hat{\xi}_\beta = M_{\beta\alpha}^{-1} B_{\alpha ij} W_{aij} K_{ab}^{-1} W_{bkl} \delta_k \delta_l. \quad (3.1)$$

Chapter 2 describes the Monte Carlo Calculation of M , K , and the product BW in real space. Notice that equation 3.1 does not indicate the space in which the calculation is performed. Because all of the data, selection functions, etc. are in real space, perform all calculations in real space until the final estimate. Then, use an FFT to obtain a Fourier space representation.

3.2.1 Calculation of $W_{bkl} \delta_k \delta_l$

The only computation involved in Equation 3.1 not discussed in Chapter 2 is the calculation of $W_{bkl} \delta_k \delta_l$. This is the only place in which the actual galaxy catalog data is introduced into the calculation. For clarity, first look at the full integral:

$$W_{bij} \delta_i \delta_j = \int \frac{\bar{n}_i \bar{n}_j \delta(r_\alpha - |\mathbf{r}_i - \mathbf{r}_j|)}{(1 + 4\pi J_{3\alpha} \bar{n}_i)(1 + 4\pi J_{3\alpha} \bar{n}_j)} \frac{n_i - \bar{n}_i}{\bar{n}_i} \frac{n_j - \bar{n}_j}{\bar{n}_j} d^3 r_i d^3 r_j \quad (3.2)$$

where $n_i = n(r_i)$. For simplicity of calculation this integral splits into three separate integrals:

$$W\delta\delta = W_{ss} - (W_{ds} + W_{sd}) + W_{dd}. \quad (3.3)$$

Where the subscript d stands for data and the subscript s stands for smooth.

$$W_{ss} = \int \frac{\bar{n}_i \bar{n}_j \delta(r_\alpha - |\mathbf{r}_i - \mathbf{r}_j|)}{(1 + 4\pi J_{3\alpha} \bar{n}_i)(1 + 4\pi J_{3\alpha} \bar{n}_j)} d^3 r_i d^3 r_j. \quad (3.4)$$

This integral is very similar to the integral for WB . The only difference is that WB has an additional factor of $\delta(r_\beta - |\mathbf{r}_i - \mathbf{r}_j|)$. This means that the calculation for WB can be used for the calculation of W_{ss} and the only modification is in the translation from continuous representation to discretized representation. When discretized, WB is a diagonal matrix whereas W_{ss} is a vector.

Because i and j are dummy indices

$$W_{sd} + W_{ds} = 2W_{ds} = 2 \int \frac{n_i \bar{n}_j \delta(r_\alpha - |\mathbf{r}_i - \mathbf{r}_j|)}{(1 + 4\pi J_{3\alpha} \bar{n}_i)(1 + 4\pi J_{3\alpha} \bar{n}_j)} d^3 r_i d^3 r_j. \quad (3.5)$$

The value n_i is not a smoothly distributed value but rather a series of delta functions at the locations of the galaxies. This means that the integral over i becomes a sum over galaxies:

$$W_{sd} + W_{ds} = 2 \sum_{\text{galaxies}(i)} \int \frac{\bar{n}_j \delta(r_\alpha - |\mathbf{r}_i - \mathbf{r}_j|)}{(1 + 4\pi J_{3\alpha} \bar{n}_i)(1 + 4\pi J_{3\alpha} \bar{n}_j)} d^3 r_j. \quad (3.6)$$

So for each galaxy, integrate over the shell centered on the galaxy's position with radius r_α . This set of 2-dimensional integrals can be performed by standard numerical techniques. It is easiest to perform this integral as the sum of integrals on the sub-shells as they intersect each of the LCRS observing areas. This is the set of integrals which takes the bulk of the computing time when calculating the term $W\delta\delta$.

The final term is

$$W_{dd} = \int \frac{n_i n_j \delta(r_\alpha - |\mathbf{r}_i - \mathbf{r}_j|)}{(1 + 4\pi J_{3\alpha} \bar{n}_i)(1 + 4\pi J_{3\alpha} \bar{n}_j)} d^3 r_i d^3 r_j. \quad (3.7)$$

Once again the values n_i and n_j are a series of delta functions at the locations of the galaxies.

So this integral should actually be written

$$\sum_{\text{galaxies}(i)} \sum_{\text{galaxies}(j \neq i)} \frac{\delta(r_\alpha - |\mathbf{r}_i - \mathbf{r}_j|)}{(1 + 4\pi J_{3\alpha} \bar{n}_i)(1 + 4\pi J_{3\alpha} \bar{n}_j)} \quad (3.8)$$

where the delta function is 1 if $r_\alpha - |\mathbf{r}_i - \mathbf{r}_j| = 0$ and 0 otherwise. Because there are essentially no galaxy pairs with exactly separation r_α , the calculation must be relaxed somewhat. In addition to this, the full calculation is using sums over discrete values (α) to approximate integrals. This means that the galaxy pair should contribute to the integral even if the separation is not equal to the arbitrary choice of α . To accommodate this, simply apply the contributions to the two values of r_α which bracketed the actual separation. The fractions (f_{lower} and f_{upper}) apportioned to each integral are reminiscent of linear interpolation:

$$f_{\text{lower}} = \frac{r_{\text{upper}} - r_{\text{sep}}}{r_{\text{upper}} - r_{\text{lower}}}, f_{\text{upper}} = \frac{r_{\text{sep}} - r_{\text{lower}}}{r_{\text{upper}} - r_{\text{lower}}}. \quad (3.9)$$

This sum can be done exactly as written with a reasonable amount of computing time. In fact, the sums can be replaced

$$\sum_{\text{galaxies}(i)} \sum_{\text{galaxies}(j \neq i)} \rightarrow 2 \sum_{\text{galaxies}(i)} \sum_{\text{galaxies}(j > i)} \quad (3.10)$$

to save half of the computing time.

Because the terms W_{ss} and $W_{sd} + W_{ds}$ are, in fact, calculated as true delta functions in α , it is necessary to reduce the value of W_{dd} so that it will contain the same volume. The delta functions mean that the volume is actually a spherical shell (with no width) with area $4\pi r_\alpha^2$. So multiply by r_α^2 and divide by

$$\int_{r_{\alpha-1}}^{r_\alpha} \left(1 - \frac{r_\alpha - r}{r_\alpha - r_{\alpha-1}}\right) r^2 dr + \int_{r_\alpha}^{r_{\alpha+1}} \left(1 - \frac{r - r_\alpha}{r_{\alpha+1} - r_\alpha}\right) r^2 dr. \quad (3.11)$$

This places all of the terms in $W\delta\delta$ on the same footing, so they can be added together. With the calculations from chapter 2, there is now a complete description of the calculation of $\hat{\xi}_\beta$ in real space.

3.2.2 Measuring the Power Spectrum

The next step is to put it all together to obtain a measurement of the power spectrum with error bars. Equation 3.1 gives the measurement of the power spectrum at wavelength k_α

marginalized over all other possible parameters. Since M is just the inverse of the covariance matrix for the parameters ξ_α , the error is given by $\sqrt{M_{\alpha\alpha}^{-1}}$. Although this gives the proper measurement at a particular wavelength (a delta function in width) this is not usually the quantity of interest. In fact, this quantity is anti-correlated. This means that neighboring points have covariances that are negative. Because neighboring points are expected to have similar values it makes sense to use a correlated measurement rather than an anti-correlated measurement. Smoothing over an appropriate window produces smaller error bars at the expense of measuring a region around k_α rather than measuring only k_α itself.

The first smoothing of interest produces what we will call the correlated spectrum. This is obtained by multiplying equation 3.1 by $M_{\gamma\beta} / \sum_\beta M_{\gamma\beta}$:

$$\hat{\xi}_\alpha^{\text{correlated}} = \frac{1}{\sum_\beta M_{\gamma\beta}} B_{\gamma ij} W_{aij} K_{ab}^{-1} W_{bkl} \delta_k \delta_l. \quad (3.12)$$

We must divide by the sum of the row of the Fisher matrix to make sure that the measurement is unbiased. Notice that this smoothes the measurement using the Fisher matrix as the smoothing function. This will correlate the data over a reasonably small width. This is a nice representation because it is the measurement that emerges most naturally from the data. Also, this measurement is nice and smooth. This is because smoothing reduces the error bars because, instead of using the measurement at just the point of interest, it averages over the surrounding points as well. In this case, the error bars are given by $\sqrt{(M_{\gamma\gamma})} / \sum_\beta M_{\gamma\beta}$. If the Fisher matrix is reasonably sharply peaked, then this representation will yield a valid, unbiased estimate of the power spectrum. In fact, most analyses use a similar weighting of the data to achieve their result. It means, however, that the measurements are not independent of one another.

The second smoothing function that produces an interesting result is obtained by using the square-root of the Fisher matrix as the smoothing function. There are many possible versions of the square-root. In this paper we diagonalize the Fisher matrix and take the square root of the Eigenvalues. This measurement is interesting because

$$\langle \Delta M^{\frac{1}{2}} \xi \Delta M^{\frac{1}{2}} \xi \rangle = 1 \quad (3.13)$$

That is to say that, smoothing with the square root of the Fisher matrix results in measurements that are uncorrelated. For this reason, we call the result decorrelated.

$$\hat{\xi}_\gamma^{\text{decorrelated}} = \frac{1}{\sum_\beta M_{\gamma\beta}^{1/2}} M_{\gamma\alpha}^{-1/2} B_{\alpha ij} W_{a ij} K_{ab}^{-1} W_{bkl} \delta_k \delta_l. \quad (3.14)$$

The errors on the measurements $\hat{\xi}_\gamma^{\text{decorrelated}}$ are just $1/\sum_\beta M_{\gamma\beta}^{1/2}$.

3.2.3 Correcting for Discrete FFT Errors

The process of using discrete matrices rather than the true continuous values leads to one other problem. The calculation of the estimates of the power spectrum is actually a calculation of the Fourier transform of the estimate of the correlation function. Taking the Fourier transform of the discretized version of the prior value of the correlation function should yield the discretized version of the prior power spectrum. However, performing this calculation actually yields a power spectrum which is lower (and at the large k end much lower) than the prior value of the power spectrum. This is because the discrete FFT of the prior power spectrum is necessarily bumpy. On the other hand, the prior correlation function (obtained using a continuous Fourier transform) is smooth. The power contained within the extra bumps are lost in the calculation. As the binning becomes finer (as more points are added) the discrepancy becomes smaller.

Fortunately, the prior value of the correlation function tells us exactly how to correct for this error. If the measured correlation function is exactly the prior correlation function, then the measured power spectrum should be exactly the prior power spectrum. This means that in order to obtain the corrected estimate of the power spectrum, take the uncorrected value of the power spectrum (before doing any smoothing) and multiply by the ratio of the prior power spectrum to the FFT of the prior discretized correlation function.

Figure 3.2 shows the results of the correction in both the 31 by 31 matrix and the 63 by 63 matrix. The dashed lines show the estimate for the power spectrum without the correction. The solid lines show the same results with the appropriate corrections applied. In both cases

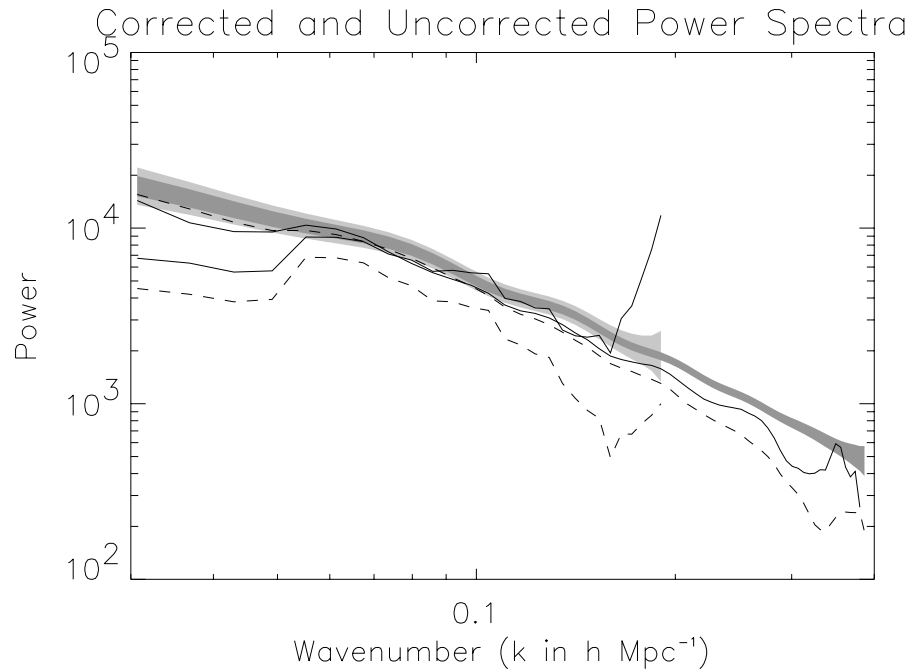


Figure 3.2: Solid lines show the correlated versions of the corrected power spectra. Dotted lines show the same versions for the uncorrected power spectra. Shaded regions show the expected ($1-\sigma$) errors.

the correction is a factor of a few at the largest k probed. Notice that the agreement between the measured power spectra becomes much better in the corrected version than it was in the uncorrected version.

3.3 Power Spectra

3.3.1 Power Spectrum of the Full LCRS

Figure 3.3 shows the correlated and decorrelated estimates of the redshift space power spectrum for the full LCRS catalog. On small scales (large k) the measured power is lower than that of the prior. On large scales, the measured power is larger than that of the prior. The correlated version (the solid line) appears to have variations that are within the expected errors. However, the decorrelated measurement has errors which are larger than expected (i.e.,

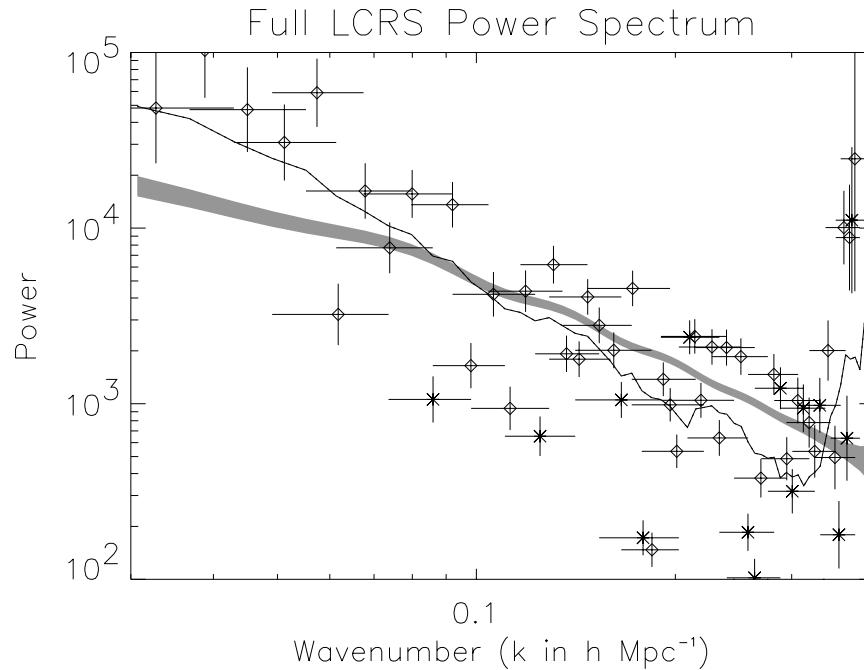


Figure 3.3: Power spectrum of all 23720 LCRS galaxies. The shaded region shows the expected deviations from the prior power spectrum for the correlated measurements. Diamonds show the measured decorrelated power for a bin with horizontal and vertical error bars. The horizontal error bars show the full width at 1/4-maximum. The position of the points is given by the center of the full width at 1/4-maximum region. Stars also show the measured power for a bin, however the measured power is negative. The solid line is the positive portion of the correlated power spectrum measurement. Notice that the scatter between points is much larger than the expected errors. This is due to the galaxies where the selection function is very small.

neighboring points are separated by much more than the error bars). The scatter is due to the large contributions from the few galaxies in sparsely sampled locations. Also, the power on the largest scales is likely to have been enhanced by these low selection function galaxies.

At locations where $k > 0.3h/\text{Mpc}^{-1}$ the estimates take a large upturn. Hamilton (2000) found that when taking the fast Fourier transform, the outer portions of a matrix are not always faithfully represented. It appears that (Figure 3.2) the last few points of the measurement are systematically too high. This means that when looking at the results, one should take the outer portions of the matrix less seriously than the middle.

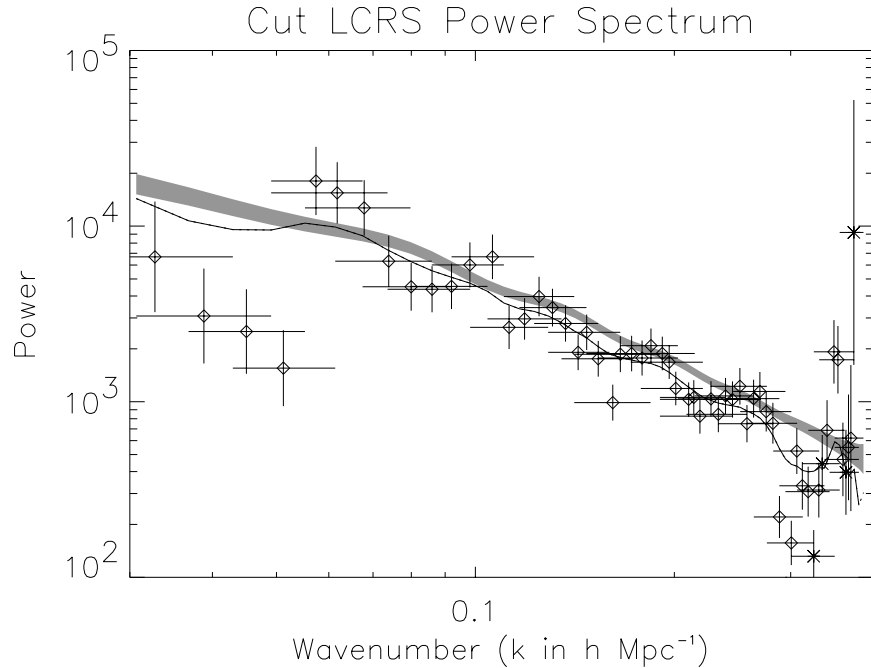


Figure 3.4: Power spectrum of the cut catalog’s 21996 LCRS galaxies. The lines and symbols are as described in Figure 3.3. Notice that the error bars are now consistent with the scatter of the points.

3.3.2 Power Spectrum of the Cut LCRS

By cutting the LCRS at $75h^{-1}$ Mpc and $475h^{-1}$ Mpc, only the region which is well fit (this eliminates the small redshift galaxies) by the Lin et al. (1996a) selection function and which is well sampled (this eliminates the most distant region) is included in the measurement. By using only the best region of the catalog, systematic errors (from a mismeasured selection function where the selection function is too low to be included in the fit to the selection function) in the measurements will be reduced. The results of this analysis are shown in Figure 3.4.

The correlated power spectrum is positive at all wavelengths. The errors in the measurement of the power spectrum using the cut catalog appear to agree with the expected level of errors. It is interesting to note that the measured power spectrum agrees rather well with the prior power spectrum (particularly in shape). The region with $k \gtrsim .3$ h Mpc⁻¹ is likely to be

inaccurate. This means that both of the negative values measured in the decorrelated power spectrum occur where it is likely to be affected by aliasing.

The prior value of the power spectrum cannot be completely ruled out by our measurement. First of all, on the largest scales (small k), redshift distortions will tend to add power to the measurement. On the very smallest scales (large k), redshift distortions will tend to reduce the measured power. Although the prior cannot be completely ruled out, it does appear that the measured power spectrum is steeper than the prior.

There is some evidence that the power spectrum is turning over at about $.06 \text{ h Mpc}^{-1}$. The region with smaller values of k is likely to be contaminated by the FFT aliasing power from larger k into the bins with smaller k . In fact, the first few measured points are not plotted due to severe aliasing problems. Unfortunately, the measurement is too insensitive to make any definitive statement about the turn-over of the power spectrum.

3.3.3 IRAS 1.2 Jy Power Spectrum

Figure 3.5 shows the measured power spectrum for the IRAS 1.2 Jy survey. Once again, the line is the pair weight measurement. The line is solid where positive. The diamonds show the canonical measurement by Fisher et al. (1993) with error bars. The stars show the power spectrum measured by the combined 1.2 Jy and QDOT surveys as measured by Tadros and Efstathiou (1995). The pair weight measurement appears to be noisier than expected. This may be due to errors in the calculation of the Fisher matrix elements. It is clear, however, that the pair weight measurement is similar to the measurements by Fisher et al. (1993) and Tadros and Efstathiou (1995).

3.3.4 Tests of the Pair Weight Method

Now that we have a power spectrum measured by the pair weight method, we would like to know the limitations of the method. The pair weight method can be tested in two additional ways. The first is to work with a data set with a known power spectrum. The second is to

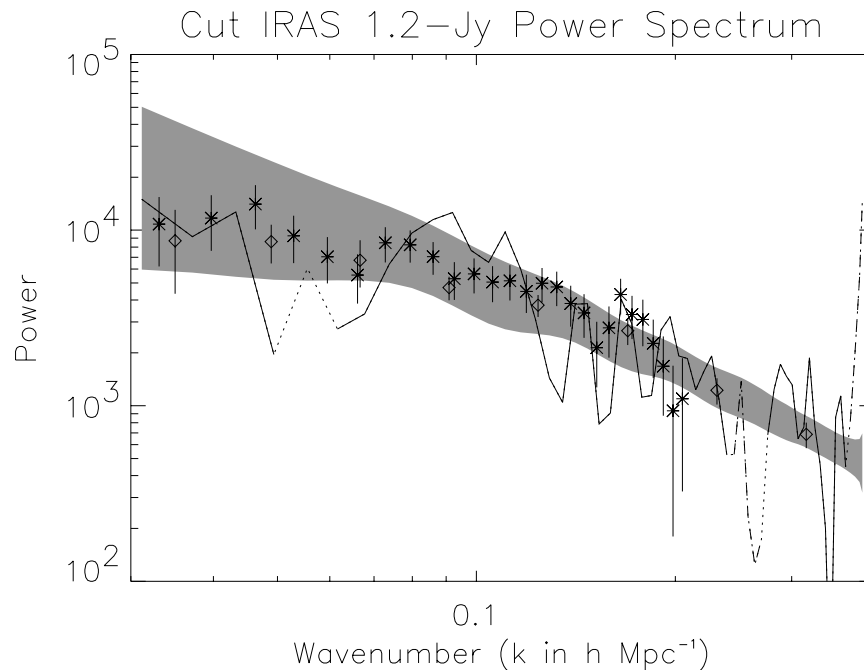


Figure 3.5: Power spectrum for IRAS 1.2 Jy catalog. The line is the pair weight measurement. The line is solid where positive, dotted where switching signs and dot-dashed where negative. Also shown are measurements by Fisher et al. (1993) (diamonds) and Tadros and Efstathiou (1995) (stars). Tadros and Efstathiou (1995) results report the power spectrum measured from the combined 1.2 Jy and QDOT surveys.

work with a prior power spectrum which is not expected to be correct to see if the selected prior affects the outcome of the measurement.

Mock Catalog with Zero Power

In order to test whether the pair weight method is able to extract the correct power spectrum from data with a known power spectrum, we tested it against a mock galaxy catalog. The mock galaxy catalog was created by randomly selecting galaxies based on the Huan Lin selection function. This means that the power spectrum (for nonzero values of k) should be zero. The results of the analysis using this mock catalog are shown in Figure 3.6. Clearly, the power measured is much smaller than the prior power spectrum. In fact the measured value in the correlated power spectrum is approximately equal to the error bar supplied on the prior. This is

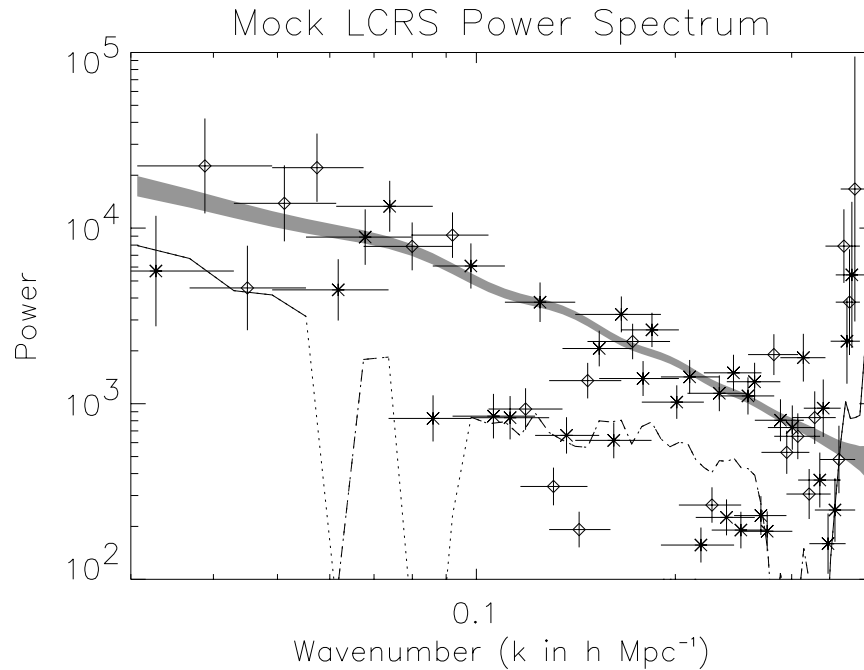


Figure 3.6: Power spectrum as measured from a mock catalog. The mock catalog has the correct selection function for the entire range of the LCRS. The input power for the catalog is zero. Here the error bars are constant in the logarithm assuming that the measured power is approximately equal to the prior power.

what one would expect. However, the measured power is systematically negative. This means that when the power in a data set is much lower than the prior value, there may be some sort of imprinting of the prior onto the data. This also says that the pair weight method, due to the errors associated with the calculation, may not measure zero all that well.

Cut LCRS with Flat Prior

When working with a prior value of the power spectrum it is important to test whether the prior value biases the calculation in some way. In other words, it is important to know that the method is measuring the data rather than measuring the prior. To test this, we used a second prior with a very different shape than that of Eisenstein and Hu (1999). We used a prior that was uniformly $10^4 (h^{-1} \text{Mpc})^3$. This prior leads to the simplest analysis. This is because the

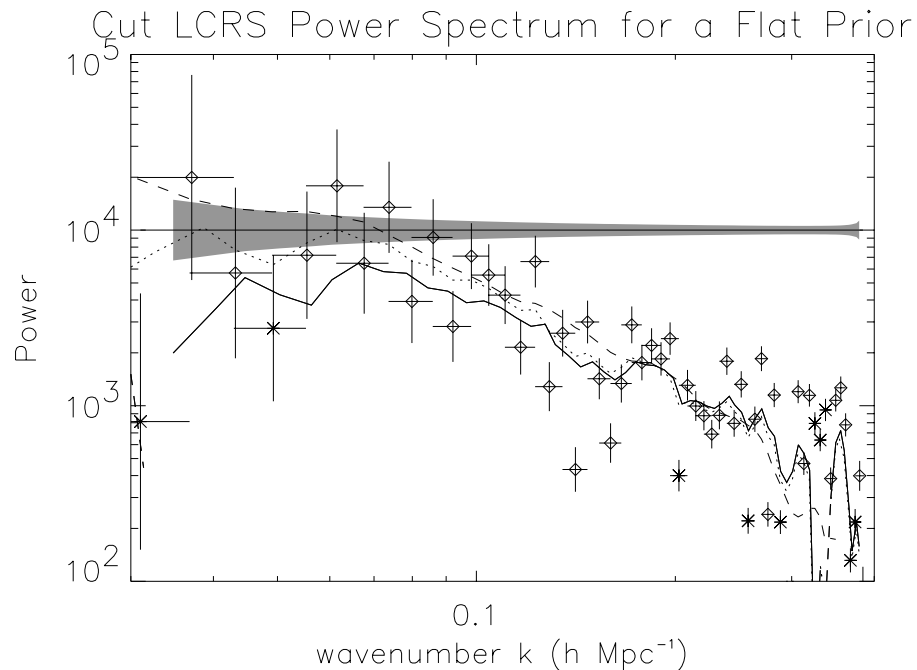


Figure 3.7: Power spectrum measured with the 21996 galaxies in the cut LCRS catalog. Again, the shaded region is the expected errors assuming the flat prior is correct. The data points (diamonds for positive and stars for negative) show the decorrelated results. The solid line is the correlated version smoothed with the typical smoothing of $\xi_{\text{prior}} M \xi_{\text{prior}}$. The dotted line is the correlated version using just the Fisher matrix M as the smoothing function. The dashed line is the result from the more realistic prior power spectrum.

Fourier transform of a flat power spectrum is a δ function. This means that our matrices become diagonal. The other benefit of the flat prior is that even when discretized the Fourier transform of the real space correlation function is still a flat power spectrum. This means that there is no discretization correction. The results from the analysis of the cut LCRS using the flat prior are shown in Figure 3.7. The measurement is positive and is consistent with the expected errors. In addition to this, the measured power is similar to that measured with the more realistic prior. On the largest scales, the flat prior measures a smaller value for the power spectrum. On the smallest scales, the flat prior measures a slightly larger value for the power spectrum. This is probably due to power shifting from locations where the power divided by the prior is high to locations where the power divided by the prior is low. This is because the smoothing function

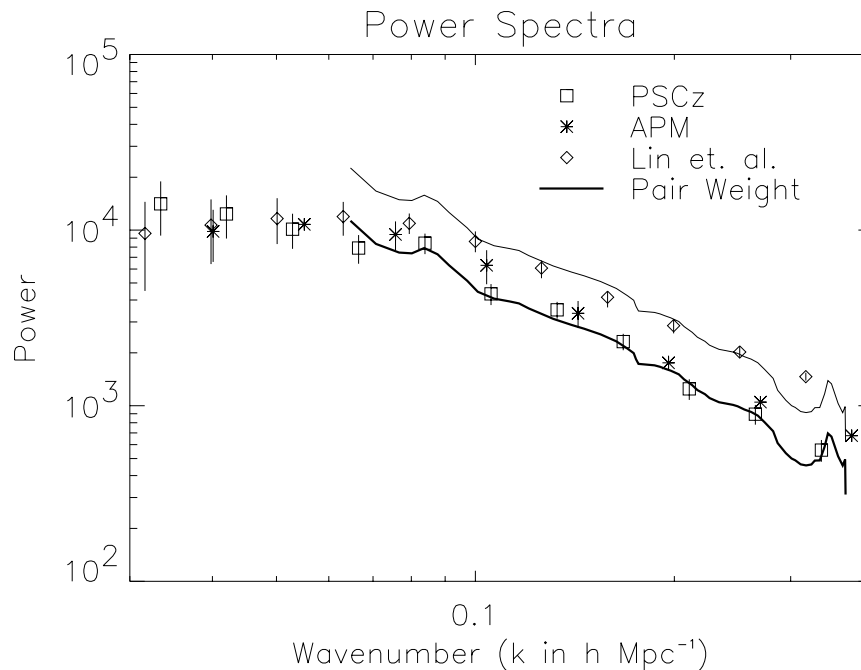


Figure 3.8: Power spectra for PSCz, APM and LCRS using different methods. The solid shows the power spectrum of LCRS measured with the pair weight method using the Eisenstein and Hu (1999) power spectrum as the prior. The diamonds and the associated error bars are the power in LCRS measured by Lin et al. (1996b). The squares and associated error bars are the power measured by Sutherland et al. (1999) from the PSCz. The stars and associated error bars are the power spectrum measured by Gaztañaga and Baugh (1998) for the APM.

($\xi_{\text{prior}} M \xi_{\text{prior}}$ where ξ_{prior} is the discretized version of the prior power spectrum, and thus not constant) assumes that the measured value of the power spectrum is close to the prior value. This is clearly false with this outrageous prior power spectrum. To correct this the dotted line shows the correlated power spectrum using M as the smoothing function. This reduces the problem. In fact, the flat prior power spectrum produces a measured power spectrum that is very similar to that measured by the more realistic power spectrum. This is a good indication that the prior power spectrum is not biasing the results.

3.3.5 Comparison of Pair Weight Results to Previous Results

Figure 3.8 shows the comparison of the Lin et al. (1996b) and the correlated measurement using the pair weight method with the Eisenstein and Hu (1999) prior. Like Lin et al. (1996b) the pair weight method shows some evidence that the power spectrum turns over at small k . Notice that the pair weight method measures smaller power than does Lin et al. (1996b), on almost all scales. However, by multiplying the result from the pair-weight method by 2, we obtain the same result as Lin et al. (1996b) over our well-measured region. It is not at all clear why two analyses should obtain results that are exactly off by a factor of 2.

Also plotted is the measurement of the power in PSCz by Sutherland et al. (1999) (squares) and the results from the APM by Gaztañaga and Baugh (1998). The pair weight method measures very nearly the same power in LCRS as Sutherland et al. (1999) does for PSCz. This result is surprising due to the fact that it is commonly believed that IRAS selected galaxies will have a smaller bias than optically selected galaxies. However, the APM results are also from an optically selected survey, and they also appear to agree with the PSCz results. This may be an indication that the bias factor of optically selected galaxies is not all that different from that of IRAS selected galaxies.

3.4 Discussion and Conclusions

In this chapter we described how to apply the pair weight method to an actual data set. We then applied the pair weight method to the Las Campanas Redshift Survey using a selection function provided by Huan Lin and a Λ CDM prior power spectrum from Eisenstein and Hu (1999). The measured power spectrum of the entire LCRS was noisier than expected. Inclusion of galaxies where the selection function is small (several galaxies are in locations where the actual selection function is zero) caused errors in the power spectrum.

We then cut the LCRS to include only the region where the selection function fit the data well. After calculating the power spectrum, we found that the discrete nature of our measure-

ment introduces errors that can be corrected. The corrected power spectrum calculated with the cut LCRS appears to be good. The fluctuations in the measurement are consistent with the expected errors. This measured power spectrum is quite similar to the prior power spectrum. The measured power spectrum was slightly larger on large scales and slightly smaller on small scales. It is possible that these differences are due to redshift distortions.

Next, we performed the pair weight calculation with a flat prior power spectrum. The measured power for the flat prior case is consistent on scales where the calculation should be accurate with the measurement using the more realistic prior. On the large scales, however, the flat prior yields lower power. This is due to power shifting from large k to small k . When smoothed over a more appropriate window the flat prior result agrees very well with the result from the more reasonable prior.

Finally the measured power spectrum was compared to other works. The power spectrum measured from LCRS using the pair weight method was lower than that measured by Lin et al. (1996b) by a factor of 2. It is not clear what causes this discrepancy in the measurement. However, our results look nearly identical to the results of Sutherland et al. (1999) from their analysis of the PSCz survey. This is surprising due to the fact that the PSCz is an IRAS selected survey which is commonly thought to be less biased than an optical survey. However, the APM, another optical catalog, has very nearly the same power spectrum (Gaztañaga and Baugh, 1998) as measured in LCRS by the pair weight method and in the PSCz survey. It appears that optically selected galaxies and IRAS galaxies may be more similar than is commonly believed.